

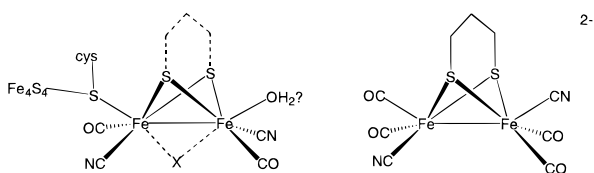
First Generation Analogues of the Binuclear Site in the Fe-Only Hydrogenases: $\text{Fe}_2(\mu\text{-SR})_2(\text{CO})_4(\text{CN})_2^{2-}$

Michael Schmidt, Stephen M. Contakes, and Thomas B. Rauchfuss*

School of Chemical Sciences
University of Illinois at Urbana–Champaign
Urbana, Illinois 61801

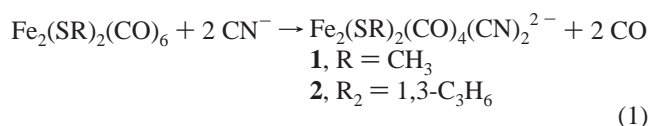
Received July 12, 1999

Hydrogenase enzymes are utilized by numerous microorganisms to produce dihydrogen or to take up dihydrogen in support of their metabolic activities. The two families of metallohydrogenases feature $\text{FeM}(\mu\text{-SR})_2(\text{CO})_n(\text{CN})_n$ cores.^{1–3} Having cyanide and CO coligands as well as metal–metal bonding, the hydrogenase active sites represent a link between the otherwise disparate realms of organometallic and biological Fe–S chemistry.^{4–6} The structure proposed⁷ for the binuclear center of the Fe-only hydrogenases is depicted on the left of the following schematic next to the molecule prepared in this study:



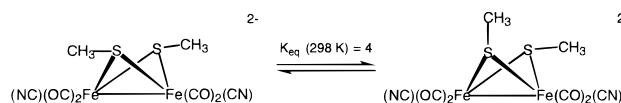
While a number of details remain uncertain, the active site structure is reproduced in crystallography of enzymes from two different genera.^{7,8}

Initial preparative efforts targeted the series $\text{Fe}_2(\text{SMe})_2(\text{CO})_{6-n}(\text{CN})_n^{n-}$. Solutions of $\text{Fe}_2(\text{SMe})_2(\text{CO})_6$ ⁹ in methanol or acetonitrile react in minutes with Et_4NCN to give exclusively $\text{Fe}_2(\text{SMe})_2(\text{CO})_4(\text{CN})_2^{2-}$ (**1**, eq 1). Analytically pure Et_4N^+ (**1a**) and Ph_4P^+ (**1b**) salts were precipitated in good yields.¹⁰ We were unable to isolate monocyano species, even when a deficiency of Et_4NCN was used, indicating that the binding of the first CN^- enhances the rate of substitution at the second metal. On the other hand, excess Et_4NCN did not lead to the formation of higher



(1)

cyanides, i.e., $\text{Fe}_2(\text{SMe})_2(\text{CO})_{6-n}(\text{CN})_n^{n-}$ ($n > 2$). Furthermore, the substitution is selective for placement of one CN^- on each Fe center, consistent with IR structural studies on the protein.¹¹ Crystallographic analysis¹² of $(\text{PPh}_4)_2[\text{Fe}_2(\text{SMe})_2(\text{CO})_4(\text{CN})_2]$ confirmed the expected connectivity but suffered from disorder due to cocrystallization of the diequatorial and axial, equatorial isomers:



An alternative approach to Fe–S–CO–CN[−] assemblies was pursued starting from $\text{Fe}_2\text{S}_2(\text{CO})_6$ because we expected to be able to effect reactions of the S–S bond after CN^- for CO substitution.¹³ This reaction afforded $(\text{NEt}_4)_2[\text{Fe}_6\text{S}_6(\text{CO})_{12}]$,¹⁴ indicating that the mildly reducing CN^- induces S-centered redox, not substitution, in contrast to the case for the $\mu\text{-SR}$ derivatives.

The crystallographic analysis of the *D. desulfuricans*-derived enzyme indicates that the Fe atoms are bridged via a 1,3-propanedithiol derivative.⁷ Such a dithiolate is constrained to the diaxial geometry, obviating problems with isomerism at the $\mu\text{-SR}$ sites.¹⁵ Red microcrystalline $(\text{NEt}_4)_2[\text{Fe}_2(\text{S}_2\text{C}_3\text{H}_6)(\text{CO})_4(\text{CN})_2]$ (**2a**, Figure 1) was obtained in 94% yield using methods for the preparation of **1a**. Compound **2a** is stable in solutions for extended periods but rapidly decomposes in air. Dynamic ¹³C NMR studies on **2a** show that the trimethylene strap inverts rapidly on the NMR time scale at room temperature. Similarly, at room temperature, we observe only one ¹³CN signal (50% enriched), while at −40 °C we observe two peaks attributed to the cessation of the ring-folding dynamics. Concomitant with the splitting of the CN[−] signals, the trimethylene CH₂ signals split into two sets at −40 °C.

Crystallographic characterization of **2a**¹⁶ confirms the resemblance of the $[\text{Fe}_2(\text{S}_2\text{C}_3\text{H}_6)(\text{CO})_4(\text{CN})_2]^{2-}$ dianion and the binuclear sites in the hydrogenases. The 1,3-propane dithiolate bridges a pair of Fe atoms, each coordinated by one CN[−] and two CO ligands. The Fe–Fe distance (2.517 Å), which is clearly bonding, is comparable to that seen for both $\text{Fe}_2(\text{SR})_2(\text{CO})_6$ derivatives^{15,17} but somewhat shorter than in both protein structures ($r_{\text{Fe-Fe}} \approx 2.6$ Å).^{7,8} The crystallography confirms the presence of one CN[−] on each Fe, as has been suggested for the *D. desulfuricans* protein.⁷ The Fe–CX (X = O vs N) distances are

- (1) Cammack, R. *Nature* **1999**, 397, 214–215.
- (2) Adams, M. W. W. *FEMS Microbiol. Rev.* **1994**, 15, 261–277.
- (3) Adams, M. W. W.; Stiefel, E. I. *Science* **1998**, 282, 1842–1843.
- (4) Volbeda, A.; Charan, M.-H.; Piras, C.; Hatchikian, E. C.; Frey, M.; Fontecilla-Camps, J. C. *Nature* **1995**, 373, 580–587.
- (5) Lai, C.-H.; Lee, W.-Z.; Miller, M. L.; Reibenspies, J. H.; Darensbourg, D. J.; Darensbourg, M. Y. *J. Am. Chem. Soc.* **1998**, 120, 10103–10114.
- (6) Amara, P.; Volbeda, A.; Carlos, J. C.; Fontecilla-Camps, J. C.; Field, M. J. *J. Am. Chem. Soc.* **1999**, 121, 4468–4477.
- (7) Nicolet, Y.; Piras, C.; Legrand, P.; Hatchikian, C. E.; Fontecilla-Camps, J. C. *Structure* **1999**, 7, 13–23.
- (8) Peters, J. W.; Lanzilotta, W. N.; Lemon, B. J.; Seefeldt, L. C. *Science* **1998**, 282, 1853–1858.
- (9) King, R. B. *J. Am. Chem. Soc.* **1962**, 84, 2460.
- (10) $(\text{PPh}_4)_2[\text{Fe}_2(\text{SCH}_3)_2(\text{CO})_4(\text{CN})_2]$ (**1b**): ¹H NMR (CD₃CN, 400 MHz) δ 1.18 (s, SCH₃, a,e), 1.71 (s, SCH₃, e,e), 1.81 (s, SCH₃, a,e) (6 H, 79% a,e, 21% e,e), 7.4–8.0 (m, PPh₄, 40 H); IR (KBr, cm^{−1}) 2073 (m), 2057 (w), 1959 (s), 1915 (vs), 1882 (s), 1863 (s), 1839 (m). Anal. Calcd for C₅₆H₄₆Fe₂N₂O₄P₂S₂ (Found): C, 64.13 (64.03); H, 4.42 (4.44); N, 2.67 (2.50). The Et_4N^+ salt (**1a**): Anal. Calcd for C₂₄H₄₆Fe₂N₄O₄S₂: C, 45.72 (45.97); H, 7.35 (7.33); Fe, 17.72 (17.59); N, 8.89 (8.98); S, 10.17 (10.34). $(\text{PPh}_4)_2[\text{Fe}_2(\text{S}_2\text{C}_3\text{H}_6)(\text{CO})_4(\text{CN})_2]$ (**2b**): ¹H NMR (CD₃CN, 400 MHz) δ 1.65 (m, SCH₂CH₂CH₂S, 2H), 1.84 (m, SCH₂CH₂CH₂S, 4H), 7.4–8.0 (m, PPh₄, 40 H); IR (KBr, cm^{−1}) 2078 (s), 2029 (w), 1951 (s), 1917 (s), 1880 (s), 1867 (sh); IR (CH₂Cl₂, cm^{−1}) 2071 (m), 2031 (w), 1964 (m), 1924 (s), 1884 (m). Anal. Calcd for C₅₇H₄₆Fe₂N₂O₄P₂S₂ (Found): C, 64.54 (64.79); H, 4.37 (4.47); N, 2.64 (2.97). The Et_4N^+ salt (**2a**): Anal. Calcd for C₂₅H₄₆Fe₂N₄O₄S₂ (Found): C, 46.74 (46.75); H, 7.22 (7.21); Fe, 17.38 (17.20); N, 8.72 (9.07); S, 9.98 (9.63). $\text{Fe}_2(\text{S}_2\text{C}_3\text{H}_6)(\text{CO})_4(\text{CN})_2 \cdot (\text{H}_2\text{O})$ (**3**): IR (KBr, cm^{−1}) 2119 (s), 2058 (s), 2038 (s), 2000 (s). Anal. Calcd for C₉H₈Fe₂N₂O₄S₂ (Found): C, 27.02 (27.15); H, 2.00 (1.89); N, 7.00 (7.26).

- (11) IR study of the *D. vulgaris* Fe hydrogenase: Pierik, A. J.; Hulstein, M.; Hagen, W. R.; Albracht, S. P. J. *Eur. J. Biochem.* **1998**, 258, 572–578.
- (12) Crystallographic details for **1b**: space group P1 (Z = 2); a = 10.7271(8), b = 12.9116(10), and c = 21.1722(16) Å, $\alpha = 80.023(2)$, $\beta = 79.553(2)$, and $\gamma = 71.198(2)^\circ$.
- (13) Seyferth, D.; Henderson, R. S.; Song, L. C. *Organometallics* **1982**, 1, 125–133.
- (14) Lilley, G. L.; Sinn, E.; Averil, B. A. *Inorg. Chem.* **1986**, 25, 1073–1075.
- (15) Winter, A.; Zsolnai, L.; Huttner, G. Z. *Naturforsch.* **1982**, 37b, 1430–1436.
- (16) Preparation of **2a**: $\text{Fe}_2(\text{S}(\text{CH}_2)_3\text{S})(\text{CO})_6$ and 2 equiv of Et_4NCN were combined at 0 °C in MeCN solution. The reaction mixture was brought to room temperature, and, after 1 h, the solvents were removed from the red solution. The residue was washed with hexanes (94% yield). Single crystals were obtained by layering CH₂Cl₂ solutions with hexanes. Crystal data for **2a**: triclinic; P1 (Z = 2); a = 7.9323(13), b = 10.0132(15), and c = 19.845(3) Å, $\alpha = 90.867(4)$, $\beta = 100.158(3)$, and $\gamma = 95.603(3)^\circ$, R₁ = 0.0636, wR₂ = 0.1592; GOF = 0.976.
- (17) Dahl, L. F.; Wei, C. H. *Inorg. Chem.* **1963**, 2, 328–334.

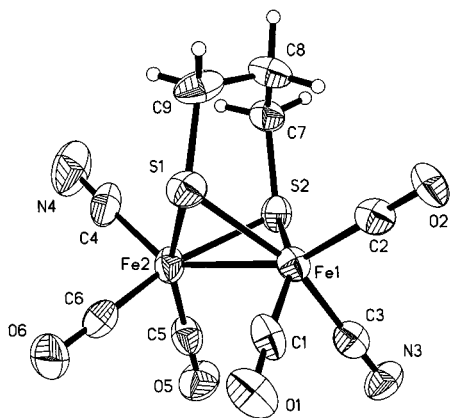


Figure 1. Structure of the dication in $(\text{Et}_4\text{N})_2[\text{Fe}_2(\text{S}_2\text{C}_3\text{H}_6)(\text{CO})_4(\text{CN})_2]$ (**2a**), with thermal ellipsoids set at the 50% probability level. Selected distances (Å) and angles (deg): Fe1–C1, 1.741(5); Fe1–C2, 1.769(6); Fe1–C3, 1.929(6); Fe1–S1, 2.2659(16); Fe1–S2, 2.2690(16); Fe1–Fe2, 2.5171(12); C1–Fe1–C2, 98.8(2); C1–Fe1–C3, 90.1(2); C2–Fe1–C3, 98.3(2); Fe1–S1–Fe2, 67.25(5); S1–Fe1–S2, 85.74(6).

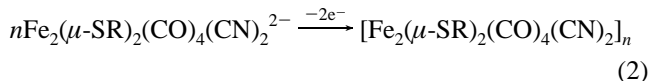
distinctly different: Fe–CO distances are ca. 0.2 Å shorter than the Fe–CN distances. It is interesting to note that the Fe–CO distances are ca. 0.08 Å shorter than in the hexacarbonyl $\text{Fe}_2(\text{SEt})_2(\text{CO})_6$. The contraction of Fe–CO distances in mixed Fe–CO/CN complexes appears to be a general phenomenon.^{5,18} The strengthening of the Fe–CO bonding by CN^- coordination may be related to the observed regioselective synthesis of **1** and **2** (see eq 1).

In contrast to the hexacarbonyls $\text{Fe}_2(\text{SR})_2(\text{CO})_6$, **2** is quite oxidatively sensitive.¹⁹ Solutions of **2** react with $(\text{NH}_4)_2\text{Ce}(\text{NO}_3)_6$ (2 equiv) or, more conveniently, I_2 (1 equiv) to give neutral $\text{Fe}_2(\text{S}_2\text{C}_3\text{H}_6)(\text{CO})_4(\text{CN})_2 \cdot \text{H}_2\text{O}$ (**3**). The oxidation of **2** to **3** was also effected, albeit less efficiently, using HOTf (2 equiv); the cogenerated H_2 (35% yield) was identified by NMR analysis (δ 4.51) and quantified by gas volume measurements. The insolubil-

(18) Hsu, H.-F.; Koch, S. A.; Popescu, C. V.; Münck, E. *J. Am. Chem. Soc.* **1997**, *119*, 8371–8372.

(19) Haines, R. J.; de Beer, J. A.; Greatrex, R. *J. Chem. Soc., Dalton Trans.* **1976**, 1749–1757.

ity of **3** and the irreversible nature of the oxidations lead us to propose that **3** is polymeric, which would be consistent with the unsaturated $32e^-$ configuration for monomeric $\text{Fe}_2(\text{S}_2\text{R})_2(\text{CO})_4(\text{CN})_2$ (eq 2). While polymeric cyanometalates are well prece-



ented (cf. Prussian Blue²⁰), redox-induced polymerization of cyanometalate monomers is uncommon and merits further study, perhaps using solubilizing thiolato ligands. Not surprisingly, and as seen in the protein,¹¹ oxidation of **2** causes a significant shift in both the ν_{CO} and ν_{CN} bands¹⁰ to higher frequencies.²¹ Compound **3** is a promising synthetic entry into the $\text{Fe}^{\text{II}}_2(\text{SR})_2\text{-CO-CN}$ manifold, as demonstrated by its reaction with imidazoles and CN^- to give soluble $\text{Fe}_2(\text{S}_2\text{C}_3\text{H}_6)\text{-CO-CN-L}$ derivatives, which will be the subject of a future report.

In summary, the electron-rich species $\text{Fe}_2(\text{S}_2\text{C}_3\text{H}_6)_2(\text{CN})_2(\text{CO})_4^{2-}$ bears a stoichiometric and structural resemblance to the Fe-only hydrogenases. The ready availability of these species should facilitate study of the molecular basis of hydrogenase catalysis.²²

Acknowledgment. This research was supported by the Department of Energy. M.S. is a recipient of a Feodor Lynen Fellowship (Alexander von Humboldt Foundation). We thank J. C. Fontecilla-Camps for helpful comments.

Note Added in Proof: Crystallographic analysis of the Fe-only hydrogenase (CpI) from *C. pasteurianum* reveals that the CO-inhibited enzyme has a $\text{Fe}(\text{CO})_2(\text{CN})$ site as seen in compounds **1** and **2** (Lemon, B. J.; Peters, J. W. *Biochemistry* **1999**, in press).

Supporting Information Available: Tables of atomic coordinates, selected bond distances and angles, thermal parameters, and selected spectroscopic and preparative details (PDF). This material is available free of charge via the Internet at <http://pubs.acs.org>.

JA9924187

(20) Dunbar, K. R.; Heitz, R. A. *Prog. Inorg. Chem.* **1997**, *45*, 283–391.

(21) Nakamoto, K. *Infrared and Raman Spectra of Inorganic and Coordination Compounds*; John Wiley: New York, 1986.

(22) Thauer, R. K.; Klein, A. R.; Hartmann, G. C. *Chem. Rev.* **1996**, *96*, 3031–3042.